PCCP

PAPER

Cite this: *Phys. Chem. Chem. Phys.*, 2017, **19**, 7352

Bonding-induced thermal transport enhancement across a hard/soft material interface using molecular monolayers†

Chao Yuan, Mengyu Huang, Yanhua Cheng and Xiaobing Luo*

Received 11th January 2017,
Accepted 7th February 2017

DOI: 10.1039/c7cp00209b

rsc.li/pccp

Manipulating thermal transport across hard/soft material interfaces is important for composites which are critical for a wide range of applications, including electronic packaging, thermal storage, sensors and medicine. To increase the interfacial thermal conductance (G_{int}), a previous strategy has focused on using a self-assembled monolayer (SAM) to bridge the phonon spectra mismatch between the materials constituting the interface. Here, we introduce a general strategy aiming for interfaces which are incompatible with the previous strategy. Copper (Cu) and epoxy resin are chosen as representative materials constituting the interface. The proposed strategy relies on using a strongly bonding SAM to covalently connect Cu and epoxy. The thermal measurements show that G_{int} can be enhanced by as much as 11 fold. An interesting result is found that the Cu/epoxy interface, modified with the SAM used in the previous strategy, shows approximate 2-fold lower G_{int}. Through a series of experiments, including tensile strength and wettability tests, the formation and characters of bonds in different interface systems are explored and understood. The correlation between bonding characters and G_{int} is also elucidated. We demonstrate that when the structure of the soft material is complex, interfacial thermal transport should be tuned by covalent bonds rather than by phonon spectra match. Finally, the great potential of the proposed strategy in manipulating the thermal properties of nanocomposites is illustrated here with a theoretical prediction.

Introduction

Assembling hard particles, such as ceramics, metals or metal oxides, into soft materials often results in large thermal resistance at the hard/soft material interface, which favors the degradation of thermal properties. Examples of particulate-filled composites whose thermal properties are impaired by interfacial resistance are numerous and range from polymer-based thermal interfaces and encapsulant materials in electronic packaging,[1–8] to nanofluids in thermal storage and sensor applications,[9,10] to nanoparticle-assisted therapeutics in medicine.[11,12] In some applications, this issue can be circumvented by organizing the particles into heterogeneous microstructures in which the particles aggregate or connect with each other to allow for rapid heat flow over the highly thermally conductive media.[13,14] However, for nanofluids, the use of large aggregates in fluids leads to a dramatic increase in viscosity, resulting in the impairment of fluidic properties.[14]

Directly tuning the interfacial thermal transport properties is a promising strategy. Phonon spectra match of the materials constituting the interface is generally recognized as a critical factor that influences interfacial thermal transport.[15] Due to their distinct compositions and bond natures, a large mismatch is usually observed in the phonon spectra of hard and soft materials, resulting in a low interfacial thermal conductance, G_{int}. A former study[16] demonstrated that bridging the acoustic mismatch between Au and an alkane-based polymer, polyethylene, with an alkanethiol self-assembled monolayer (SAM) can greatly enhance G_{int}. Polyethylene and the alkanethiol SAM have very similar chemical compositions, which enables a favorable acoustic match. However, for other commonly used soft materials with complex structures, like epoxy resin, it is quite difficult to obtain similarly structured SAMs to match their phonon spectra.

Theoretical studies[17–19] also suggest that G_{int} can be tailored by an order of magnitude by controlling the interfacial bond energy. Such an idea has been put into practice in inorganic solid/solid[20,21] and solid/water interfaces[22,23] by chemically introducing a strongly bonding SAM. However, this unique control of interfacial bonds and thermal transport properties has less often been achieved in practice at hard/soft interfaces. In addition, although the nexus between G_{int} and interfacial

State Key Laboratory of Coal Combustion, School of Energy and Power Engineering, Huazhong University of Science and Technology, Wuhan 430074, China.
E-mail: luoxb@hust.edu.cn

† Electronic supplementary information (ESI) available. See DOI: 10.1039/c7cp00209b

bonds has been clarified through solid/water interfaces,[22,23] the formation and characters of the bonds are yet to be explored or understood.

Here, we experimentally demonstrate that the G_{int} of a hard/soft material interface can be significantly enhanced by introducing a strongly bonding SAM. Copper (Cu) and epoxy resin are chosen as representative hard and soft materials, respectively. The measurement results show that G_{int} can be enhanced by as much as 11 fold by the proposed strategy. To study the correlation between interfacial bond energy and G_{int}, we create another interface system where the SAM is chosen to be of the alkanethiol type adopted in ref. 16. Through a series of characterization techniques, we explore the formation and characters of the bonds in the two interface systems. Finally, a theoretical prediction is made to show the great importance of our proposed strategy in manipulating the thermal transport properties of nanocomposites.

Results and discussion

Synthesis of interface systems

As illustrated in Fig. 1a and b, Cu/epoxy interfaces were created by dispersing spherical Cu microspheres into an epoxy resin solution and consolidating the suspending fluids (see Experimental section). To achieve interfaces with SAM connection, the Cu microspheres were firstly modified with SAMs (see Fig. 1a) using a chemical solution deposition method (see Experimental section). We build two Cu/SAM/epoxy systems by varying the SAM's end-group functionalities (schematically shown in Fig. 1c). The first system employs 11-amino-1-undecanethiol hydrochloride (SAM-NH_2), and the other employs an alkanethiol type SAM (dodecanethiol, SAM-CH_3), which is adopted in ref. 16. Both SAMs possess the thiol functionality (–SH) at the ω-end permitting strong bonding of the molecules to the Cu surface. Different α-end-group chemistries (–CH_3, –NH_2) ensure large variations in bond strength

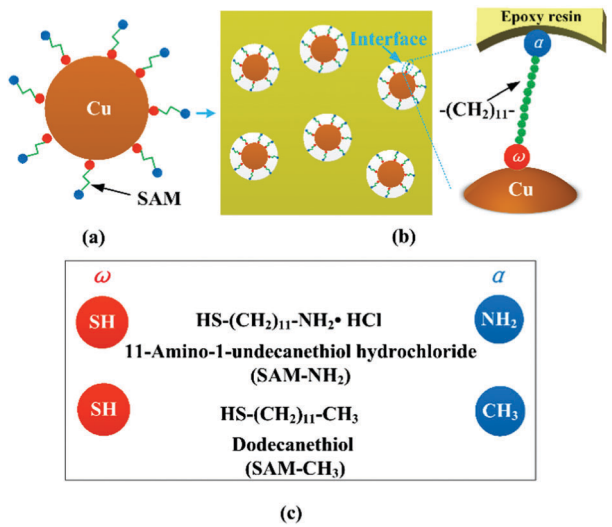

Fig. 1 Depiction of (a) a Cu surface modified with a SAM and (b) Cu/SAM/epoxy systems; (c) list of SAM chemistries studied and abbreviations used in the text.

at the SAM/epoxy interface. The –NH_2 group is expected to provide strong covalent bonds, and weak van der Waals bonds will be provided by the –CH_3 group.

Measurement of interfacial thermal conductance

The Cu/SAM/epoxy systems are assumed to be homogenously embedded in the epoxy-based composites. In this study, the G_{int} of the systems was evaluated by fitting the measured thermal conductivity data of the composites to the results predicted by an analytical model. A great number of models[2,24–28] have shown that the thermal conductivity of two-component homogeneous composites is determined by the intrinsic properties of the fillers and the matrix, the geometry and loading of the fillers, and G_{int}. For spherical particles, one of the most prominent models is the modified Bruggeman asymmetric model (MBAM) which is expressed as:[28]

$$(1-f)^3 = \left(\frac{k_m}{k_{eff}}\right)^{(1+2\beta)/(1-\beta)} \left(\frac{k_{eff}-k_p(1-\beta)}{k_m-k_p(1-\beta)}\right)^{3/(1-\beta)} \quad (1)$$

where k_{eff} is the effective thermal conductivity of the composite; k_m and k_p are the matrix and filler thermal conductivities, respectively; f is the volume fraction of the filler; β is called the Kapitza radius defined as:

$$\beta = \frac{k_m}{G_{int}d/2} \quad (2)$$

where d is the filler diameter. When the dispersed phase is much more conducting than the matrix ($k_p/k_m \gg 1$), eqn (1) can be simplified and written as:

$$k_{eff} = \frac{k_m}{(1-f)^{3(1-\beta)/(1+2\beta)}} \quad (3)$$

The Cu/epoxy composite is very suitable as a simplified case considering that epoxy has very low conductivity and Cu has very high conductivity (the values are given in Table S1 in the ESI†).

Therefore, according to eqn (2) and (3), G_{int} can be extracted once k_{eff} is measured and other variables are obtained (see Experimental section). Fig. 2a gives the fitting results for the Cu/epoxy, Cu/SAM-NH_2/epoxy and Cu/SAM-CH_3/epoxy systems and Fig. 2b provides the evaluated values. The G_{int} of the Cu/epoxy interface is extracted to be 12.5 MW m^{-2} K^{-1}. It is of the same order as the G_{int} of other hard/soft interfaces dominated by weak van der Waals interaction, such as carbon nanotube/organic solvent (~12 MW m^{-2} K^{-1}),[29] hexagonal boron nitride/epoxy (13.2 MW m^{-2} K^{-1}),[30] gold/hexadecane (28 MW m^{-2} K^{-1})[16] and gold/paraffin wax (25 MW m^{-2} K^{-1})[16] interfaces. Functionalizing the Cu/epoxy interface with SAM-NH_2 obviously enhances the G_{int}. The G_{int} is improved from 12.5 MW m^{-2} K^{-1} to 142.9 MW m^{-2} K^{-1}, exhibiting a more than 11-fold increase. It is interested to note that in comparison with Cu/epoxy, the interface modified with SAM-CH_3 shows an approximately 2-fold lower G_{int}, 7.1 MW m^{-2} K^{-1}.

Characterization of interfacial bonds

It is generally believed that the enhancement of G_{int} results from the formation of covalent bonds at both the Cu/SAM-NH_2

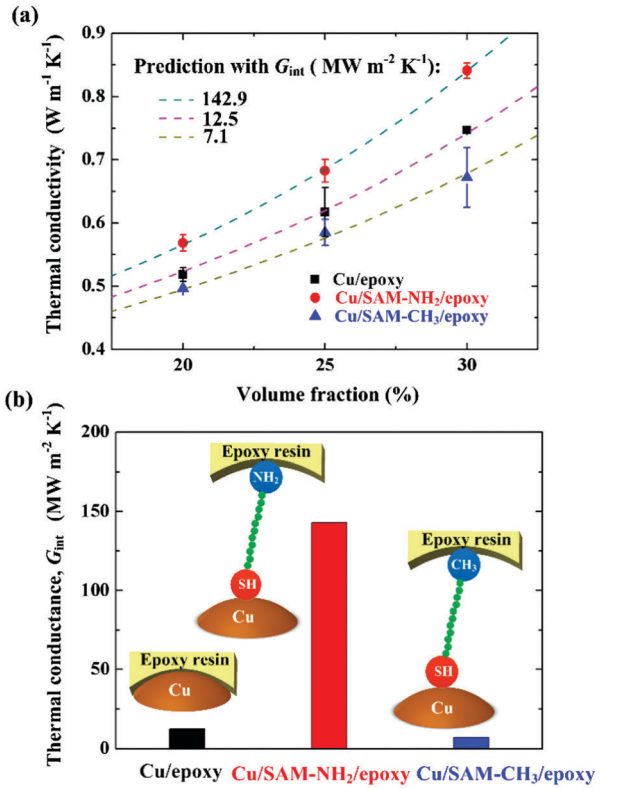

Fig. 2 (a) Data fitting to extract the G_{int} of the Cu/epoxy, Cu/SAM-NH_2/epoxy and Cu/SAM-CH_3/epoxy systems. Dots: measured thermal conductivity of the composites; colored dashed lines: thermal conductivity predicted by the modified Bruggeman asymmetric model (MBAM).[28] (b) Extracted results of G_{int}.

and SAM-NH_2/epoxy interfaces. We conduct independent experimental measurements to characterize the bonds and elucidate their formation. In addition, for the Cu/SAM-CH_3/epoxy system, although covalent bonds are believed to occur between thiols and Cu, the SAM-CH_3/epoxy interfacial interaction should be still of the van der Waals type according to the low G_{int}. Therefore, we also experimentally verify the bond type at such an interface.

The presence of chemically bonded thiols on Cu is verified by FESM and XPS (see Experimental section). Fig. 3a and d, Fig. 3b and e and Fig. 3c and f provide the surface topography of Cu microspheres before and after modification with SAM-NH_2 and SAM-CH_3. The images with higher magnification show that the SAMs modify the Cu with nanomesh structures (Fig. 3e) or nanoparticles (Fig. 3f). These nanostructures bundle together covering the whole microspheres.

Fig. 3g gives the XPS spectra of pure microspheres and microspheres treated with SAMs. In comparison with the control spectrum, significantly higher S and N content is measured in the SAM-NH_2 treated sample and a higher S content is measured in the SAM-CH_3 treated sample. Due to spin–orbit splitting, the S 2p peaks are separated into S $2p_{3/2}$ and S $2p_{1/2}$ components. As discussed in the literature,[31] for free alkanethiol SAMs, the S $2p_{3/2}$ component should appear at 163.5–163.8 eV, whereas, for alkanethiols chemisorbed on Cu, the S $2p_{3/2}$ peak will move downward to ~162 eV. Fig. 3h and i provide the measured high

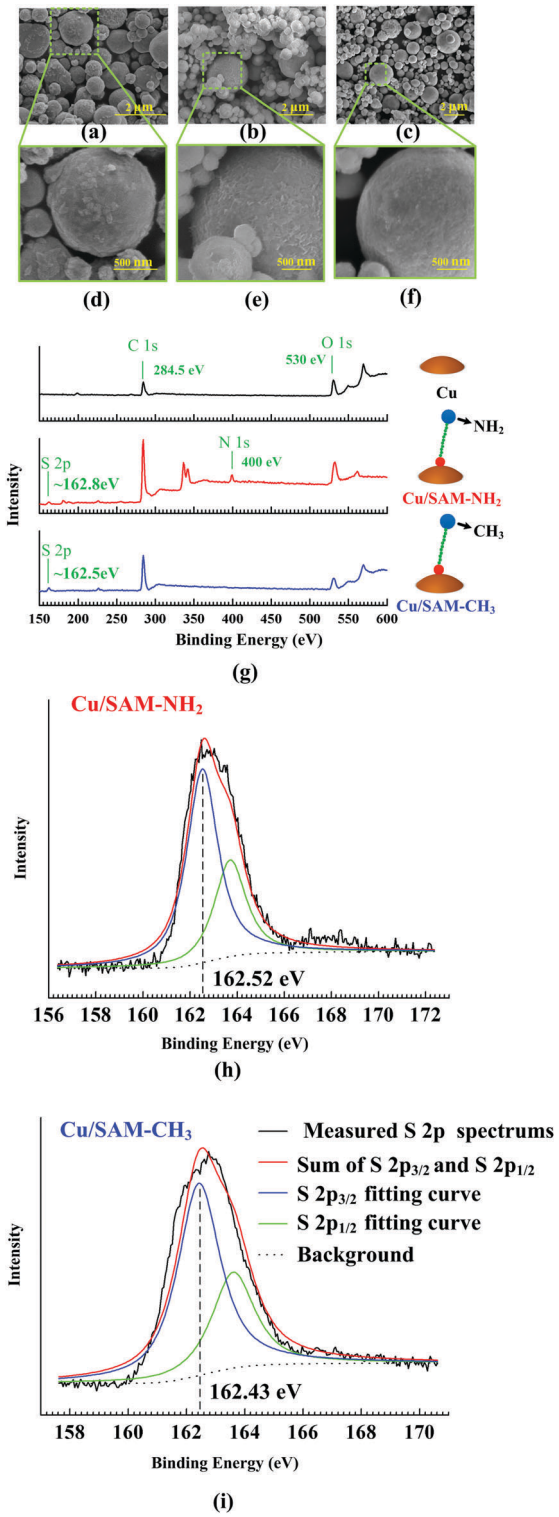

Fig. 3 FESM images of (a and d) pure Cu, (b and e) SAM-NH_2 modified Cu and (c and f) SAM-CH_3 modified Cu. (g) XPS spectra of pure Cu and Cu treated with SAMs. High resolution S 2p spectra of (h) SAM-NH_2 and (i) SAM-CH_3 modified Cu, and the corresponding fitting curves of S $2p_{3/2}$ and S $2p_{1/2}$.

resolution S 2p spectra of the SAM-NH_2 and SAM-CH_3 modified Cu, and the corresponding fitting curves of S $2p_{3/2}$ and S $2p_{1/2}$

(the fitting method is introduced in the Experimental section). The S $2p_{3/2}$ components are observed at 162.52 eV and 162.43 eV, which compare very well with the typical S $2p_{3/2}$ binding energy of alkanethiols chemisorbed on Cu. This XPS analysis suggests that chemically bonded thiols are present on Cu.

Next, the mechanism of S–Cu formation is analyzed. Since Cu modification experiments were conducted in an ambient environment, Cu was oxidized before reacting with the SAMs. As discussed in the literature,[32] the oxidized surfaces of Cu are still active for the chemisorption of alkanethiols. In addition, Keller and Ron's studies[33,34] proved that the oxide formed on the Cu surface can be reduced to metallic Cu by –SH, and its reactions can result in the formation of chemisorbed copper thiolate layers. The most likely oxide on the Cu surface is Cu_2O,[32,34,35] so the reaction can be described by the equation:[34,36]

$$2RSH + Cu_2O \rightarrow 2RSCu(surface) + H_2O \quad (4)$$

where R represents $NH_2(CH_2)_{11}$ and $(CH_2)_{12}$ for SAM-NH_2 and SAM-CH_3, respectively.

Compared to Cu–S bonds, it is more difficult to characterize the bonds at SAM/epoxy interfaces, since they are embedded in the composites. We adopted tensile strength tests[37–39] to conduct a qualitative analysis of the interfacial bonds. As schematically shown in Fig. 4a, tensile strength tests are applied on the composite samples (see Experimental section). The measured results for Cu/epoxy, Cu/SAM-NH_2/epoxy and Cu/SAM-CH_3/epoxy composites are 29.79 MPa, 48.17 MPa and 31.53 MPa, respectively (Fig. 4b). Compared to the Cu/epoxy composite, Cu/SAM-NH_2/epoxy exhibits 61.7% larger tensile strength. The enhanced tensile property is attributed to the interaction between SAM-NH_2 and the epoxy compound during composite polymerization. While interacting with epoxy, the alkane chains extend and expose the –NH_2 groups to the epoxy molecules. Fig. 4c illustrates the nucleophilic reaction between SAM-NH_2 treated Cu and a novolac epoxy, which was proposed and proved by experiments in ref. 36. The reaction shows that the –NH_2 group in SAM-NH_2 opens the oxirane ring in novolac epoxy, forming a secondary amine with covalent bonds. In contrast, there is no obvious enhancement in tensile strength for the composite modified with SAM-CH_3, although Cu is covalently bonded with the S molecule. The poor tensile property is a consequence of the non-polar nature of the SAM-CH_3 molecule.[36] The non-polar tail (–CH_3) hinders the formation of hydrogen bonds with the ingredients inside the epoxy, resulting in a weak van der Waals interaction between them.

For some solid/liquid interfaces,[22,23] the wettability of the liquid on the solid material is used to characterize the interfacial bonding energy. A thermodynamic parameter, W_{SL}, expresses the relationship between the bonding energy and surface wettability (or contact angle):[22,23]

$$W_{SL} = \gamma_{AW}(1+\cos\theta) \quad (5)$$

where γ_{AW} is the air/liquid surface tension and θ is the contact angle. According to eqn (5), low θ means strong interfacial bonding. Thus, we characterized the interfacial bonding energy by measuring the θ of fluidic epoxy resin on surfaces before and after modification with SAM-NH_2 and SAM-CH_3 (see Experimental section). As shown in Fig. 4d, the surface consisting of pure Cu microspheres has a θ of 19.9°, whereas the SAM-NH_2 treated surface exhibits a much lower θ (~11°). The θ of the SAM-NH_2 treated surface was also measured in ref. 40 and exhibited a much smaller value (6.6°). Conversely, the wettability of SAM-CH_3

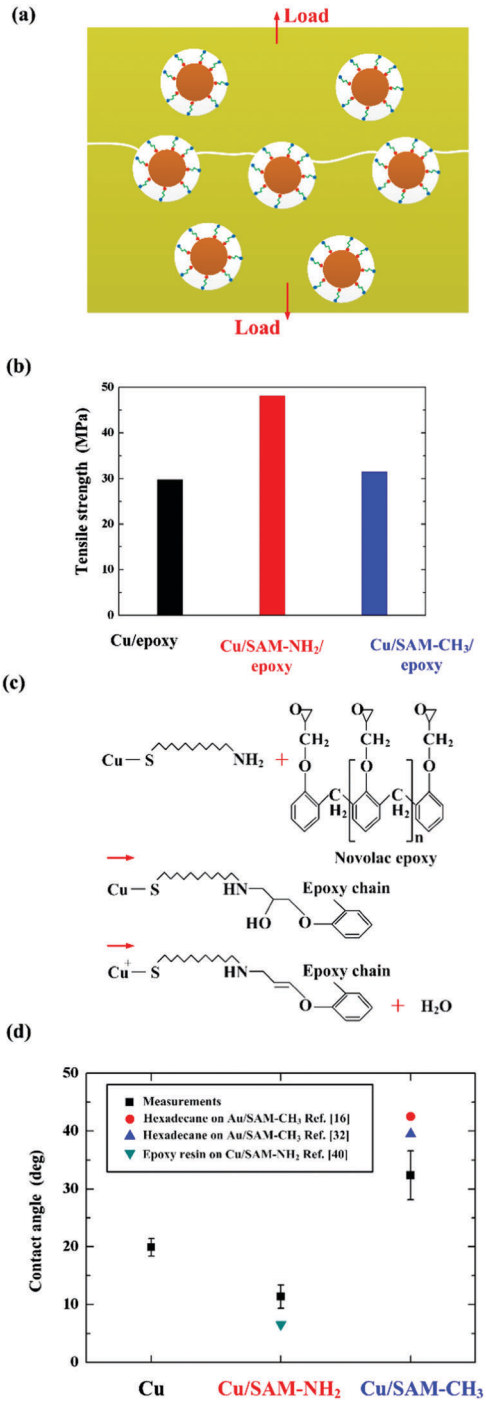

Fig. 4 (a) Schematic of the tensile test. (b) Measured tensile strength of Cu/epoxy, Cu/SAM-NH_2/epoxy and Cu/SAM-CH_3/epoxy composites. (c) Nucleophilic reaction between SAM-NH_2 treated Cu and a novolac epoxy. (d) Contact angle of polymeric materials (epoxy, hexadecane) on the pure and SAM modified surfaces.

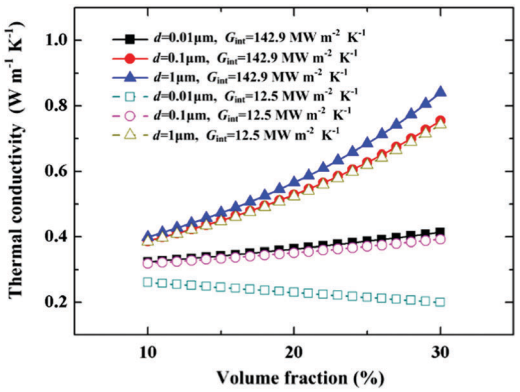

Fig. 5 Predicted thermal conductivities of Cu/epoxy and Cu/SAM-NH_2/ composites *versus* volume fraction at different Cu diameters.

treated surfaces is poorer than that of the other two surfaces. The θ was measured to be 32.4°. Fig. 4d also presents the θ of another polymeric material, hexadecane,[16,32] on SAM-CH_3 treated surfaces. The large values demonstrate that the wettability is poor, too. The wettability tests consolidate the conclusions that interfacial bonding is stronger at the SAM-NH_2/epoxy interface and weaker at the SAM-CH_3/epoxy interface.

The simulation results obtained in ref. 36 support our experimental observations. Using molecular dynamics (MD) simulations, the interfacial bonding energy is calculated for Cu/epoxy, and Cu/epoxy modified with cystamine dihydrochloride and hexadecanethiol. The calculated results are 0.535 J m^{-2}, 0.838 J m^{-2} and 0.055 J m^{-2}, respectively. The structures and chemistry of cystamine dihydrochloride and hexadecanethiol are similar to those of SAM-NH_2 and SAM-CH_3, respectively. All of them have the thiol functionality (–SH), a long alkane chain in the middle, and –CH_3 or –NH_2 at the α-end. The simulation results prove the existence of covalent bonds between Cu and epoxy when Cu is modified with an amine SAM, instead of an alkanethiol SAM.

Importance of covalent bonds

For solid/water interfaces,[22,23] researchers have found that G_{int} increases directly with interfacial bonding energy. The same tendency is found for the Cu/epoxy interface. However, the G_{int} at some weak bonded interfaces (Au/alkanethiol SAM/polyethylene) is not decreased but enhanced significantly.[16] The reason has been explained in the Introduction. The acoustic match between the two components makes thermal transport efficient. As for the SAM-CH_3/epoxy interface, their phonon spectra cannot match, since there is an obvious distinction between the structures of the two components. Therefore, when the structure of the soft material is complex, the enhancement of G_{int} should be induced by covalent bonds rather than by the acoustic match.

Manipulation of the thermal properties of nanocomposites

We demonstrate the great potential of our proposed strategy in manipulating the thermal properties of nanocomposites. Two types of Cu/epoxy composites are investigated. One is assumed to be modified with SAM-NH_2 (G_{int} = 142.9 MW m^{-2} K^{-1}) and another is assumed to be without any surface modification (G_{int} = 12.5 MW m^{-2} K^{-1}). Fig. 5 gives the predicted thermal conductivities of the composites at different Cu microsphere diameters. The results show that for the 30 vol% composite without modification, the thermal conductivity decreases from 0.74 W m^{-1} K^{-1} to 0.39 W m^{-1} K^{-1} by 47.3%, and to 0.20 W m^{-1} K^{-1} by 73.0%, when the diameter of 1 μm decreases by 10 and 100 times, respectively. In particular, the thermal conductivity of the 10 nm Cu filled composite will not increase with volume fraction due to the low G_{int}. While, after the surface modification with SAM-NH_2, the extent to which the thermal conductivity decreases with diameter is weakened. The percentage of reduction decreases down to 10.7% and 51.2%, respectively. Thus, with the dimension decreasing to the nanosize, filling the soft matrix with high loading particles will not contribute to the thermal conductivity any more. While, functionalizing the interfaces inside the composites with strongly bonding SAMs will relieve the adverse impact of interfacial thermal resistance on thermal conductivity.

Conclusions

In summary, we have demonstrated an effective strategy to tune thermal transport across hard/soft material interfaces. The proposed strategy relies on using a strongly bonding SAM to covalently connect hard and soft materials. The thermal measurements show that for the Cu/epoxy interface, G_{int} can be enhanced by as much as 11 fold. Moreover, this study experimentally illustrates that when the structure of the soft material is complex, interfacial thermal transport should be tuned by covalent bonds rather than by phonon spectra match. We emphasize the great potential of our proposed strategy in material design for heat transfer-critical applications like electronic packaging, thermal storage, sensors and medicine.

Experimental section

Materials

Cu microspheres, with an average diameter of 1 μm, were purchased from Alfa Aesar. Epoxy resin, supplied by Huntsman, is composed of a low viscosity bisphenol-A based liquid resin (Araldite LY1564) and an amine based hardener (Aradur 3487). The mixing ratio is 100 : 34 by weight when used. The properties of copper and epoxy resin, such as density, heat capacity, thermal diffusivity and thermal conductivity, are summarized in Table S1 in the ESI.† SAMs, dodecanethiol (SAM-CH_3) and 11-amino-1-undecanethiol hydrochloride (SAM-NH_2), were purchased from Aldrich. They were used without further purification.

Cu modification with SAMs

SAMs were assembled on Cu surfaces by a chemical solution deposition method (see details in supplementary note 1 in the ESI†). The general procedures involve immersing the Cu microspheres in an ethanolic solution of 1 mM SAM and stirring

them for a sufficient amount of time. Prior to use, all SAM treated samples were rinsed thoroughly with ethanol and air dried.

Cu/SAM/epoxy system formation

Cu/SAM/epoxy systems were formed by fabricating the epoxy-based composites with randomly dispersed modified microspheres. The modified microspheres were first suspended in the fluidic epoxy. The resulting suspension was mechanically stirred for 20 min to be fully dispersed. Subsequently, the suspension was sent into a vacuum chamber to remove the bubbles introduced during the mixing step. After that, the polymer suspension was cast into Teflon molds. They were heated at 100 °C for 1 h and 150 °C for 2 h to obtain the fully cured composite samples. Using the described method, the Cu/SAM-CH_3/epoxy and Cu/SAM-NH_2/epoxy composites were prepared with Cu volume fractions of 20, 25 and 30 vol%, respectively. For comparison, Cu/epoxy composites were also prepared with the same volume fractions.

Evaluation of interfacial thermal conductance G_{int}

G_{int} was evaluated by fitting the measured thermal conductivity data of the composites to the results predicted by the MBAM.[28]

Thermal conductivity was measured according to the formula: $k = \alpha C_p \rho$, where C_p, ρ and α are the effective heat capacity, density and thermal diffusivity of the composites, respectively. The evaluation of effective C_p and ρ is introduced in supplementary note 2 in the ESI.† The effective α was measured by a laser flash apparatus (LFA467, Netzsch) at 25 °C. The data of effective C_p, ρ, α and k are summarized in Table S2 (ESI†).

For the MBAM (eqn (2) and (3)), k_m, f_{cop} and d are input as known parameters. Now, G_{int} is the only unknown parameter in the prediction of k_{eff}. Fig. S1 (ESI†) provides the predicting results of k_{eff} at different values of G_{int}. Then, G_{int} can be extracted by fitting the measured thermal conductivity to one of the predicting curves (see details in supplementary note 3 in the ESI†).

Characterization

The surface topography of SAM treated Cu microspheres was evaluated by field-emission scanning electron microscopy (FESM, FEI Sirion-200). To investigate the surface composition, X-ray photoelectron spectroscopy (XPS, Axis-Ultra DLD-600W) was utilized. The XPS spectra are calibrated with respect to the C 1s peak (284.5 eV). When analyzing the S 2p spectrum, the S 2p peak is separated into S $2p_{3/2}$ and S $2p_{1/2}$, due to spin–orbit splitting. The S $2p_{3/2}$ and S $2p_{1/2}$ splitting peaks are obtained by the curve fitting method using XPSPEAK software. Some parameters in this method are set as follows: an approximate 2 : 1 relative area separated by 1.18 eV with an equal L–G% and FWHM level.

The tensile properties of the composites were measured at room temperature by means of a universal materials testing machine (Zwick, Z010). All composite samples were prepared using the same procedure as described. A schematic of the tensile test is shown in Fig. S2 (ESI†).

The static contact angles of epoxy resin on SAM treated surfaces were measured. The surfaces were prepared by laying the microspheres on a glass substrate with a thickness of ~2 mm. 5 μL of epoxy resin droplets was gently deposited on the surfaces using a microsyringe. A picture of the droplet was taken by using a digital camcorder until the droplet became stable. The obtained pictures were analyzed for the contact angle using ImageJ software (NIH). For each sample, three images (six angles) were taken to obtain the average value.

Acknowledgements

This work was supported by the National Science Foundation of China (51625601 and 51576078). The authors would like to thank Ms Gao Xianhui, Mr Huang Qingwu and Mr Yang Wenbing for assistance with FSEM imaging, XPS and tensile strength tests, respectively.

Notes and references

1 R. S. Prasher, J. Shipley, S. Prstic, P. Koning and J. L. Wang, *ASME J. Heat Transf.*, 2003, **125**, 1170–1177.
2 R. S. Prasher, *Proc. IEEE*, 2005, **94**, 1571–1586.
3 X. B. Luo, R. Hu, S. Liu and K. Wang, *Prog. Energy Combust. Sci.*, 2016, **56**, 1–32.
4 C. Yuan, B. Duan, L. Li, B. Xie, M. Y. Huang and X. B. Luo, *ACS Appl. Mater. Interfaces*, 2015, **7**, 13000–13006.
5 C. Yuan, B. Xie, M. Y. Huang, R. K. Wu and X. B. Luo, *Int. J. Heat Mass Transfer*, 2016, **94**, 20–28.
6 C. Yuan, L. Li, B. Duan, B. Xie, Y. M. Zhu and X. B. Luo, *Int. J. Therm. Sci.*, 2016, **102**, 202–209.
7 A. L. Moore and L. Shi, *Mater. Today*, 2014, **17**, 163–174.
8 X. M. Sun, H. Sun, H. P. Li and H. S. Peng, *Adv. Mater.*, 2013, **25**, 5153–5176.
9 R. Zheng, J. Gao, J. Wang and G. Chen, *Nat. Commun.*, 2011, **2**, 289.
10 D. Wen, G. Lin, S. Vafaei and K. Zhang, *Particuology*, 2009, **7**, 141–150.
11 J. A. Barreto, W. O'Malley, M. Kubeil, B. Graham, H. Stephan and L. Spiccia, *Adv. Mater.*, 2011, **23**, H18.
12 X. Huang, I. H. El-Sayed, W. Qian and M. A. El-Sayed, *J. Am. Chem. Soc.*, 2006, **128**, 2115–2120.
13 R. Prasher, W. Evans, P. Meakin, J. Fish, P. Phelan and P. Keblinski, *Appl. Phys. Lett.*, 2006, **89**, 143119.
14 W. Evans, R. Prasher, J. Fish, P. Meakin, P. Phelan and P. Keblinski, *Int. J. Heat Mass Transfer*, 2008, **51**, 1431–1438.
15 E. T. Swartz and R. O. Pohl, *Rev. Mod. Phys.*, 1989, **61**, 605.
16 F. Sun, T. Zhang, M. M. Jobbins, Z. Guo, X. Zhang, Z. Zheng, D. Tang, S. Ptasinska and T. Luo, *Adv. Mater.*, 2014, **26**, 6093–6099.
17 L. Hu, L. Zhang, M. Hu, J. S. Wang, B. Li and P. Keblinski, *Phys. Rev. B: Condens. Matter Mater. Phys.*, 2010, **81**, 235427.
18 M. Hu, P. Keblinski and P. K. Schelling, *Phys. Rev. B: Condens. Matter Mater. Phys.*, 2009, **79**, 104305.
19 R. Prasher, *Appl. Phys. Lett.*, 2009, **94**, 041905.

20 M. D. Losego, M. E. Grady, N. R. Sottos, D. G. Cahill and P. V. Braun, *Nat. Mater.*, 2012, **11**, 502–506.
21 P. J. O'Brien, S. Shenogin, J. Liu, P. K. Chow, D. Laurencin, P. H. Mutin, M. Yamaguchi, P. Keblinski and G. Ramanath, *Nat. Mater.*, 2013, **12**, 118–122.
22 N. Shenogina, R. Godawat, P. Keblinski and S. Garde, *Phys. Rev. Lett.*, 2009, **102**, 156101.
23 H. Harikrishna, W. A. Ducker and S. T. Huxtable, *Appl. Phys. Lett.*, 2013, **102**, 251606.
24 C. W. Nan, R. Birringer, D. R. Clarke and H. Gleiter, *J. Appl. Phys.*, 1997, **81**, 6692–6699.
25 A. Devpura, P. Phelan and R. Prasher, *Nanosc. Microsc. Therm.*, 2001, **5**, 177–189.
26 L. Li, H. Zheng, C. Yuan, R. Hu and X. B. Luo, *Heat Mass Transfer*, 2016, **52**, 2813–2821.
27 D. Ganapathy, K. Singh, P. Phelan and R. Prasher, *ASME J. Heat Transf.*, 2005, **127**, 553–559.
28 A. G. Every, Y. Tzou, D. P. H. Hassleman and R. Raj, *Acta Metall. Mater.*, 1992, **40**, 123–129.
29 S. T. Huxtable, D. G. Cahill, S. Shenogin, L. Xue, R. Ozisik, P. Barone, M. Usrey, M. S. Strano, G. Siddons, M. Shim and P. Keblinski, *Nat. Mater.*, 2003, **2**, 731–734.
30 Z. Y. Lin, Y. Liu, S. Raghavan, K. S. Moon, S. K. Sitaraman and C. P. Wong, *ACS Appl. Mater. Interfaces*, 2013, **5**, 7633–7640.
31 T. P. Ang, T. S. A. Wee and W. S. Chin, *J. Phys. Chem. B*, 2004, **108**, 11001–11010.
32 P. E. Laibinis, G. M. Whitesides, D. L. Allara, Y. T. Tao, A. N. Parikh and R. G. Nuzzo, *J. Am. Chem. Soc.*, 1991, **113**, 7152–7167.
33 H. Keller, P. Simak, W. Schrepp and J. Dembowski, *Thin Solid Films*, 1994, **244**, 799–805.
34 H. Ron, H. Cohen, S. Matlis, M. Rappaport and I. Rubinstein, *J. Phys. Chem. B*, 1998, **102**, 9861–9869.
35 Y. S. Gong, C. Lee and C. K. Yang, *J. Appl. Phys.*, 1995, **77**, 5422–5425.
36 C. K. Wong, H. Fan and M. M. Yuen, *IEEE Trans. Compon. Packag. Technol.*, 2008, **31**, 297–308.
37 H. Xu, X. Zhang, D. Liu, C. Yan, X. Chen, D. Hui and Y. Zhu, *Composites, Part B*, 2016, **93**, 244–251.
38 J. Zang, Y. J. Wan, L. Zhao and L. C. Tang, *Macromol. Mater. Eng.*, 2015, **300**, 737–749.
39 K. Liu, X. Zhang, H. Takagi, Z. Yang and D. Wang, *Composites, Part A*, 2014, **66**, 227–236.
40 C. K. Wong and M. M. Yuen, *59th Electronic Components and Technology Conference*, San Diego, CA, 2009, pp. 1816–1823.

